

## Research report

## Decreased brain interstitial fluid dynamics is associated with risk of Alzheimer's disease-related cognitive decline

Yihao Guo<sup>a</sup>, Tao Liu<sup>b,\*</sup>, Huijuan Chen<sup>a</sup>, Liangdong Zhou<sup>c</sup>, Weiyan Huang<sup>a</sup>, Kun Zhang<sup>b</sup>, Xiaoyi Wang<sup>a</sup>, Yi wang<sup>d,e</sup>, Juan Helen Zhou<sup>f</sup>, Feng Chen<sup>a,\*\*</sup>, for the Alzheimer's Disease Neuroimaging Initiative

<sup>a</sup> Department of Radiology, Hainan General Hospital (Hainan Affiliated Hospital of Hainan Medical University), Haikou, China

<sup>b</sup> Department of Neurology, Hainan General Hospital (Hainan Affiliated Hospital of Hainan Medical University), Haikou, China

<sup>c</sup> Department of Radiology, Brain Health Imaging Institute (BHII), Weill Cornell Medicine, New York, NY, USA

<sup>d</sup> Department of Biomedical Engineering, Cornell University, Ithaca, NY 14853, USA

<sup>e</sup> Department of Radiology, Weill Cornell Medical College, New York, NY 10065, USA

<sup>f</sup> Centre for Sleep and Cognition, Yong Loo Lin School of Medicine, National University of Singapore, Singapore

## ARTICLE INFO

## Keywords:

Diffusion tensor parameter

Glymphatic function

Alzheimer's disease

Cognitive decline

## ABSTRACT

**Background:** Diffusion-tensor image analysis along the perivascular space (ALPS) index that has the potential to reflect brain interstitial fluid (ISF) dynamics may predict the development of Alzheimer's Disease (AD). We aimed to study whether brain ISF dynamics indicated by the ALPS index relate to AD dementia diagnosis and AD-related changes.

**Methods:** This study included a discovery cohort ( $n = 180$ ) and a validation cohort ( $n = 127$ ), which were composed of cognitively normal, subjective memory concern, mild cognitive impairment, and AD dementia subjects. All participants underwent brain magnetic resonance imaging examination and neuropsychological evaluation. The diffusivities and diffusion-tensor image analysis along the perivascular space (ALPS) were calculated. The support vector machine (SVM) model for AD dementia diagnosis was built in the discovery cohort and validated in the validation cohort. Linear mixed-effects models were used to evaluate the association between the ALPS and cognitive decline. Cox regression models were used to evaluate the association between the ALPS and the risk of AD dementia.

**Results:** There was a lower median ALPS index in the AD dementia group compared to other groups (all  $P < 0.05$ ) for both cohorts. The SVM model for AD dementia diagnosis produced an AUC of 0.802 in the discovery cohort ( $P < 0.001$ ) and 0.783 in the external validation cohort ( $P < 0.001$ ). Higher ALPS levels were associated with less cognitive decline ( $P < 0.001$ ). Moreover, lower baseline ALPS had a greater risk of converting to AD dementia ( $P = 0.014$ ).

**Conclusions:** The SVM model based on diffusivities and ALPS was effective for AD dementia diagnosis, and higher ALPS levels are associated with a lower risk of AD-related changes. These findings suggest that ALPS may provide a useful AD progression or treatment biomarker.

## 1. Introduction

Alzheimer's disease (AD) is the leading cause of dementia and is rapidly becoming one of the most costly, lethal, and burdensome diseases of this century (Scheltens et al., 2021). The most widely accepted

explanation for AD pathogenesis is the amyloid cascade hypothesis, which suggests that AD is primarily initiated by the accumulation of  $\beta$ -amyloid ( $A\beta$ ) peptides into senile plaques. This is followed by the accumulation of phosphorylated tau (pTau) proteins into neurofibrillary tangles, leading to subsequent neuronal loss and cognitive decline

\* Correspondence to: Department of Neurology, Hainan General Hospital (Hainan Affiliated Hospital of Hainan Medical University), No. 19, Xiuhua St, Xiuying Dic, Haikou, Hainan 570311, China

\*\* Correspondence to: Department of Radiology, Hainan General Hospital (Hainan Affiliated Hospital of Hainan Medical University), No. 19, Xiuhua St, Xiuying Dic, Haikou, Hainan 570311, China

E-mail addresses: [ltao829@163.com](mailto:ltao829@163.com) (T. Liu), [fenger0802@163.com](mailto:fenger0802@163.com) (F. Chen).

<https://doi.org/10.1016/j.brainresbull.2025.111295>

(Karran et al., 2011; Jack et al., 2013, 2018). The abnormal deposition of A $\beta$  and pTau in AD is closely associated with the dysfunction of the glymphatic system, which is responsible for clearing protein waste from the brain (Oshio, 2023). Mouse models have shown that the glymphatic system contributes to 55–65 % of A $\beta$  clearance from the brain (Iliff et al., 2012), and impairment of downstream meningeal lymphatic vessels reduces the clearance of extracellular tau protein from the brain parenchyma (Cao et al., 2018; Patel et al., 2019).

In recent years, several magnetic resonance imaging (MRI) methods have been developed to evaluate glymphatic function in the human brain (Taoka and Naganawa, 2020a). Direct visualization of the glymphatic flow system has been achieved through MRI tracer studies using intrathecal injections of gadolinium-based contrast agents (GBCA) (Iliff et al., 2013; Eide and Ringstad, 2015), although this approach is not practical for routine clinical use or research (Taoka and Naganawa, 2020b). Alternative methods, such as GBCA-free cerebrospinal fluid fraction mapping, can measure glymphatic fluid, but this technique is not yet widely applied in clinical settings (Zhou et al., 2024). The GBCA-free diffusion tensor image (DTI) analysis along the perivascular space (ALPS) technique (Taoka et al., 2017; Hsu et al., 2023; Haller et al., 2024) can estimate the interstitial fluid (ISF) dynamics and partially reflect the activity of the glymphatic system. Previous studies have demonstrated that the ALPS index correlates with intrathecal GBCA glymphatic measurements (Zhang et al., 2021). However, limited research has been conducted to validate the association between the ALPS index and cognitive function across different cohorts, and no studies have investigated the relationship between the ALPS index and cognitive decline over time.

In this study, we aimed to investigate the association between ISF dynamics, as indicated by the ALPS index, and cognitive function. We analyzed two independent cohorts representing a broad spectrum of AD, examining whether the ALPS index is related to AD dementia diagnosis, cognitive decline, and the risk of developing AD dementia.

## 2. Methods

### 2.1. Participants

This study selected two sets of independent data from the Alzheimer's Disease Neuroimaging Initiative (ADNI) and the Chinese Tropical Population Cohort Study on Healthy Aging and Dementia (CTPCS-HEAD). The ADNI was launched in 2003 as a public-private partnership, led by Principal Investigator Michael W. Weiner, MD; the related protocols can be found online ([www.adni-info.org](http://www.adni-info.org)). The CTPCS-HEAD is an ongoing population-based study cohort, launched in 2022 from a tropical region of Hainan Island, Southern China. CTPCS-HEAD participants are followed annually for the development of MCI and dementia. Written informed consent was obtained for all participants from ADNI participants and the CTPCS-HEAD cohort, and the study procedures were approved by the institutional review board at each of the participating centers.

Participants were classified as individuals with AD dementia based on the National Institute of Neurological and Communicative Disorders and Stroke and the Alzheimer's Disease and Related Disorders Association (NINCDS-ADRDA) criteria (McKhann et al., 2011) and mild cognitive impairment (MCI) based on reduced cognitive performance often involving memory, representing a high-risk state for the development of AD (Albert et al., 2011; Bondi et al., 2014). Cognitively normal (CN) was diagnosed based on the exclusion of MCI and dementia, requiring a CDR score of 0, no obvious emotional problems, and normal education-adjusted scores in the MMSE and the memory subdomain. A subset of the participants from both cohorts had cognitively normal older adults with subjective reports of cognitive changes, as named subjective memory concern (SMC), which was no informant-based complaint of memory impairment or decline, and normal cognitive performance on the MMSE and the memory

subdomain.

All ADNI2 and ADNIGO participants, two subsets of ADNI, who underwent DTI and three-dimensional (3D) T1 image examinations were initially selected ( $n = 245$ ). All participants were between the ages of 55 and 90 years and had no significant neurologic disease other than AD. Fifty-four participants who did not have CSF samples taken were excluded, resulting in 191 participants. Baseline CSF A $\beta$ 42, A $\beta$ 40, and pTau levels for each participant were obtained from the ADNI depository (Bittner et al., 2016). CSF A+ was based on CSF A $\beta$ 42 levels with a cutoff value of  $\leq 880$  pg/ml, and CSF T+ was based on CSF pTau levels with a cutoff value of  $\geq 26.64$  pg/ml (Bucci et al., 2021).

A total of 137 participants selected from CTPCS-HEAD were recruited. The inclusion criteria were (1) between 55 and 90 years, (2) right handedness, (3) without other neurologic diseases or organ failure, and (4) did not have ongoing alcohol or substance misuse. Each participant underwent brain MRI scans and blood sampling. The blood samples were collected and analyzed according to a standardized protocol. In addition, the plasma A $\beta$ 42, A $\beta$ 40, and pTau concentrations were measured using two single-molecule array kits (Simoa; Quanterix, Billerica, MA, USA), as previously described (Li et al., 2022).

The demographic characteristics, including age, sex, education, and APOE4 states were collected for all participants. Neuropsychological assessments were performed, including the Mini-Mental State Examination (MMSE) as a measure of global cognition, Clinical Dementia Rating (CDR), and Functional Activities Questionnaire (FAQ) as measures of daily functioning. The CDR sum of boxes (CDR-SB) scores were used to evaluate disease severity.

### 2.2. Brain MRI acquisition

All participants from the ADNI cohort underwent whole-brain MRI examination on a 3 T GE Medical Systems scanner. The DTI data were acquired along 41 gradient directions for  $b = 1000$  s/mm<sup>2</sup> and 5 images for  $b = 0$  s/mm<sup>2</sup>, with an echo planar imaging sequence with TR = 13,000 ms, TE = 68.7 ms, matrix size =  $256 \times 256$ , FOV =  $350 \times 350$ , number of slices = 59, slice thickness = 2.7 mm, no gap, and number of excitations = 1 (Mayo et al., 2017). The 3D T1W images were acquired with a spoiled gradient echo sequence using the following parameters: TR = 400 ms, TE = 2.8 ms, flip angle =  $11^\circ$ , and voxel size =  $1 \times 1 \times 1.2$  mm<sup>3</sup> (Basaia et al., 2019).

In the CTPCS-HEAD, all participants underwent a whole-brain MRI examination on a 3 T Siemens scanner (Magnetom Prisma) with a 64-channel head/neck received coil. The DTI data were acquired along 64 gradient directions for  $b = 1000$  s/mm<sup>2</sup> and 12 images for  $b = 0$  s/mm<sup>2</sup>, with a simultaneous multi-slice echo planar imaging sequence with TR = 4500 ms, TE = 65 ms, matrix size =  $112 \times 112$ , FOV =  $224 \times 224$  mm<sup>2</sup>, number of slices = 74, slice thickness = 2 mm, no gap, and number of excitations = 1. The 3D T1W images were acquired with magnetization-prepared rapid acquisition gradient echo sequence using the following parameters: TR = 2300 ms, TE = 2.26 ms, TI = 900 ms, flip angle =  $8^\circ$ , and voxel size =  $1 \times 1 \times 1$  mm<sup>3</sup>.

### 2.3. Image analysis

According to previous studies (Taoka et al., 2017; Hsu et al., 2023), the ALPS index associated with glymphatic function was defined as follows:

$$\text{ALPS index} = \frac{\text{mean}(D_{x\text{proj}}, D_{x\text{assoc}})}{\text{mean}(D_{y\text{proj}}, D_{z\text{assoc}})} \quad (1)$$

Where,  $D_{x\text{proj}}$  and  $D_{y\text{proj}}$  represent the x-axis and y-axis diffusivities in the area of projection fibers and  $D_{x\text{assoc}}$  and  $D_{z\text{assoc}}$  represent the x-axis and z-axis diffusivities in the area of the association fibers. A higher ALPS index indicates better glymphatic function. Diffusion metric images were generated using the DSI studio program. To avoid bias due to

manually drawn region of interest (ROI), an atlas-based approach was used in this study (Yokota et al., 2019). Briefly, each subject's FA map was coregistered to the FA map template of the ICBM-DTI-81 atlas by nonlinear registration using SPM12 (<http://www.fil.ion.ucl.ac.uk/spm/>). The subject's other diffusion metric maps were warped based on the registration matrix of the FA map. Aligned with a previous study (Hsu et al., 2023), the ROIs of projection and association fiber on the left hemisphere were selected using the ICBM-DTI-81 atlas. To avoid the effect of white matter microstructure impairment on ALPS index calculation, voxels with FA values less than 0.3 were excluded from the ROIs (Kamagata et al., 2022; Benítez et al., 2018). The ALPS index was computed automatically according to Eq. (1).

Individual 3D T1W image processing was performed using SPM12 and its extension toolbox (CAT12, <https://neuro-jena.github.io/cat/>). The T1W images were normalized using the standard Montreal Neurological Institute (MNI) template. To obtain the gray matter volume (GMV) ratio for each participant, we calculated the total modulated GMV and then divided it by the individual total intracranial volume.

## 2.4. Outcomes

The primary outcome was the AD diagnosis using radiomic method. The diffusivities (Dzproj and Dzassoc) with significant differences between the AD dementia and non-AD dementia (CN, SMC, and MCI) groups for both cohorts and the ALPS index were selected as radiomic features. With these three features, the support vector machine (SVM) model was trained and 5-fold cross-validated for AD diagnosis in the ADNI cohort and externally validated in the CTPCS-HEAD cohort. For the SVM model, radial basis function and sequential minimal optimization method were applied. The secondary outcome was the longitudinal change in cognition, as measured by the MMSE scale in the ADNI cohort. MMSE is a cognitive test that is highly relevant to cognitive changes and is often used as a basis for making a clinical diagnosis or for inclusion in clinical trials. The clinical outcome was the prediction of progression to AD dementia at any time during longitudinal follow-up. Clinical status was evaluated according to the clinical diagnosis and recorded at each follow-up visit by a physician experienced in dementia disorders.

## 2.5. Statistical analysis

The statistical analyses were performed using SPSS 20.0 software and R programming language (version 4.0.0, R Foundation for Statistical Computing, Vienna, Austria). All significance tests were 2-sided with  $\alpha = 0.05$  as the significance threshold. Clinical data between the CN, SMC, MCI, and AD dementia groups were compared using the Kruskal-Wallis test and the  $\chi^2$  test. Differences in the diffusivities and ALPS index between the four groups were compared using the Kruskal-Wallis test followed by a post hoc Dunnett T3 test. The diffusivities and ALPS index were compared according to the conversion status during follow-up using the Mann-Whitney *U* test. Partial correlation analyses were done to investigate the relationship between the ALPS index and neuropsychological scores for both cohorts after adjusting age, sex, education, and APOE4. Univariate linear regression was used to model the associations between the diffusivities, ALPS index, and AD biomarkers for both cohorts. The receiver operating characteristic (ROC) curve was applied to assess the performance of the developed model of AD diagnosis both for training and validation. Furthermore, linear mixed-effects (LME) modeling was used to assess the association of baseline ALPS index levels (adjusted for age, sex, education, and APOE4) with the study outcome of longitudinal change in the MMSE score in various A $\beta$  and tau profiles. LME models used an interaction term between ALPS index and time as a independent variable, and the MMSE score was used as a dependent variable. Confounding variables including age, sex, education, and APOE4 were adjusted as fixed effect in these LME models with random intercept and slope for each patient. We further control

GMV ratio in addition to the original confounding variables to study the relationships between ALPS index levels and longitudinal change in the MMSE score. Finally, Cox regression modeling was used to assess the association between ALPS index and conversion to AD dementia during longitudinal follow-up.

## 3. Results

### 3.1. Cohort characteristics

In the ADNI cohort, 4 participants with incomplete DTI data and 7 participants with severe distortion on DTI were excluded. According to their clinical diagnosis (Aisen et al., 2015; Petersen et al., 2010), the subjects were grouped CN (*n* = 35), SMC (*n* = 28), MCI (*n* = 82), and AD dementia (*n* = 35). The general characteristics of the study population across diagnostic groups are shown in Table 1. There were no significant group differences in age or education, but a significant difference did exist in sex (*p* = 0.026). The MCI and AD groups had a higher prevalence of APOE4 carriers than the CN and SMC groups. Moreover, the AD group had the lowest CSF A $\beta$ 42 and A $\beta$ 40 levels and highest CSF pTau level. There were lower GMV ratios in patients with AD. The median follow-up time was 60 months, with 84.25 % of participants having at least a 2-year visit and 65.7 % having at least a 4-year visit. At follow-up, 27 participants from MCI group had progressed to AD dementia.

In the CTPCS-HEAD cohort, 10 participants with head motion in DTI data were excluded. According to their clinical diagnosis (Aisen et al., 2015; Petersen et al., 2010), the subjects were grouped CN (*n* = 25), SMC (*n* = 51), MCI (*n* = 32), and AD dementia (*n* = 19). Table 2 shows the general characteristics of the study population across diagnostic groups are shown in Table 2. There were no significant group differences in sex, but significant differences existed in age (*p* = 0.034) and education (*p* < 0.001). Similar to the ADNI cohort, the MCI and AD groups had a higher prevalence of APOE4 carriers than the CN and SMC groups. In addition, the AD group had the highest plasma pTau level and the lowest plasma A $\beta$ 42 level. Lower GMV ratios were found in patients with AD.

### 3.2. Group difference in ALPS index and diffusion-tensor parameters

The median ALPS index according to the participant groups for both cohorts is shown in Fig. 1. The median ALPS index was lower in the AD dementia group than in CN (*P* < 0.001 for the ADNI cohort and *P* = 0.002 for the CTPCS-HEAD cohort), SMC (*P* = 0.023 for the ADNI cohort and *P* < 0.001 for the CTPCS-HEAD cohort), and MCI groups (*P* = 0.023 for the ADNI cohort and *P* = 0.008 for the CTPCS-HEAD cohort) for both cohorts. There was no significant difference between CN and SMC groups (*P* = 0.404), CN and MCI groups (*P* = 0.525), and SMC and MCI groups (*P* = 0.099) for the CTPCS-HEAD cohort. Significant differences between CN and MCI groups (*P* < 0.001) and between CN and SMC groups (*P* = 0.018) were observed in ADNI cohorts.

The median diffusivity according to the participant groups for both cohorts is summarized in Table 3. In the ADNI cohort, diffusivities along the x-axis and z-axis in the projection neural fibers showed differences among the groups (*P* < 0.001 and *P* = 0.046, respectively). Meanwhile, diffusivities along the z-axis in the association neural fibers also showed differences among the groups (*P* = 0.001). In the CTPCS-HEAD cohort, diffusivities along the y-axis and z-axis in the projection neural fibers showed differences among the groups (*P* < 0.001 and *P* = 0.002, respectively). Meanwhile, diffusivities along the y-axis in the association neural fibers also showed differences among the groups (*P* < 0.001).

### 3.3. Correlation between ALPS index and cognition

Partial correlation analyses were performed between the ALPS index and neuropsychological scores for both cohorts independently (Fig. 2),

**Table 1**  
General subject characteristics in ADNI cohort.

Characteristic	CN (n = 35)	SMC (n = 28)	MCI (n = 82)	AD dementia (n = 35)	P Value
Age, y	73 (60 – 89)	73.5 (66 – 83)	74 (55 – 88)	75 (64 – 90)	0.782
Sex, female/male*	18/17	18/10	29/53	12/23	<b>0.026</b>
Education, y	16 (12 – 20)	16.5 (12–20)	16 (11–20)	16 (9–20)	0.453
APOE4 positive*	10	10	46	22	<b>0.007</b>
CSF Aβ42 (pg/ml)	1345 (351 –2612)	1185 (416 – 2966)	828 (337 – 2529)	576 (255 – 1340)	<b>&lt; 0.001</b>
CSF Aβ40 (pg/ml)	8325 (5048–11417)	8445 (3513–14983)	8220 (4138–14342)	6767 (2946–15475)	<b>0.017</b>
CSF pTau (pg/ml)	19.27 (9.86–31.12)	19.26 (8.53–45.64)	22.22 (9.22–76.51)	30.36(10.77–74.51)	<b>&lt; 0.001</b>
GMV ratio (%)	0.44 (0.39 – 0.48)	0.43 (0.38 – 0.48)	0.42 (0.31 – 0.48)	0.40 (0.34 – 0.45)	<b>&lt; 0.001</b>
CDR-SB	0 (0 – 0)	0 (0 – 0.5)	1.0 (0.5 – 3.5)	4.5 (1.0 – 8)	<b>&lt; 0.001</b>
MMSE	29 (24 – 30)	29 (24–30)	28 (24–30)	24 (20–26)	<b>&lt; 0.001</b>
FAQ	0 (0 – 3)	0 (0–7)	1 (0–22)	13 (1–28)	<b>&lt; 0.001</b>
Follow up missing	0	0	5	6	
Converted to AD dementia, n	3	1	27	NA	
Time under risk of AD dementia, months	78 (6–120)	75 (6–108)	48 (3–120)	NA	

Note: Unless otherwise specified, data are medians, with ranges in parentheses.  
\* Data are the number of participants.

**Table 2**  
General subject characteristics in CTPCS-HEAD cohort.

Characteristic	CN (n = 25)	SMC (n = 51)	MCI (n = 32)	AD dementia (n = 19)	P Value
Age, y	68 (55 – 81)	68 (55 – 78)	71 (58 – 81)	74 (55 – 90)	<b>0.034</b>
Sex, female/male*	13/12	36/15	17/15	11/8	0.294
Education, y	14 (9 – 22)	15 (9–24)	13 (3–18)	12 (0–19)	<b>0.001</b>
APOE4 positive*	3	9	13	8	<b>0.015</b>
Plasma Aβ42 (pg/ml)	5.29 (2.09 – 8.37)	6.04 (2.20 – 9.02)	5.43 (2.87 – 7.64)	4.70 (2.19 – 6.60)	<b>0.026</b>
Plasma Aβ40 (pg/ml)	82.26 (50.04–103.68)	87.99 (62.08 – 110.72)	91.53 (58.56 – 123.66)	84.32 (51.67 – 134.10)	0.178
Plasma pTau (pg/ml)	1.42 (0.80 – 3.79)	1.94 (0.48 – 4.84)	2.08 (1.22 – 5.79)	3.53 (2.29 – 6.31)	<b>&lt; 0.001</b>
GMV ratio (%)	0.42 (0.39 – 0.47)	0.43 (0.39 – 0.46)	0.41 (0.36 – 0.45)	0.39 (0.35 – 0.44)	<b>&lt; 0.001</b>
CDR-SB	0 (0 – 0)	0 (0 – 0.5)	10.5 (0 – 0.5)	1.0 (1.0 – 3)	<b>&lt; 0.001</b>
MMSE	29 (27 – 30)	29 (24–30)	26.5 (22–30)	19 (14–27)	<b>&lt; 0.001</b>
FAQ	0 (0 – 1)	0 (0–5)	0.5 (0–8)	8 (0–28)	<b>&lt; 0.001</b>

Note: Unless otherwise specified, data are medians, with ranges in parentheses.  
\* Data are the number of participants.

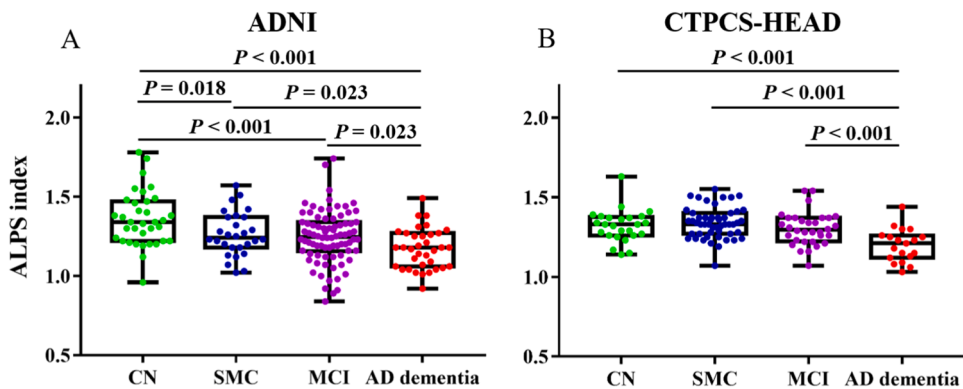


**Fig. 1.** Distribution of ALPS index across diagnostic groups in (A) ADNI and (B) CTPCS-HEAD cohorts.

controlling for age, sex, education, and APOE4. For both cohorts, the ALPS index was positively correlated with the MMSE score (Fig. 2A&D) and was negatively correlated with CDR-SB (Fig. 2B&E) and FAQ (Fig. 2C&F).

**3.4. Association between ALPS index, diffusion-tensor parameters, and AD biomarkers**

The associations between the ALPS index and AD biomarkers are summarized in Table 4. The CSF Aβ42 levels were significantly associated with the ALPS index, and there was no association between the CSF

pTau or CSF Aβ40 level and the ALPS index. Plasma Aβ42 and pTau levels were significantly associated with the ALPS index, while there was no association between plasma Aβ40 level and the ALPS index. Additionally, diffusivity along the y-axis in the association neural fibers was associated with CSF Aβ42, plasma Aβ42, and plasma pTau levels, and diffusivity along the z-axis in the projection fibers was associated with CSF Aβ42, CSF Aβ40, and plasma pTau levels. Plasma pTau levels were also associated with diffusivities along x-axis and z-axis in the projection fibers and along z-axis in the association fibers.

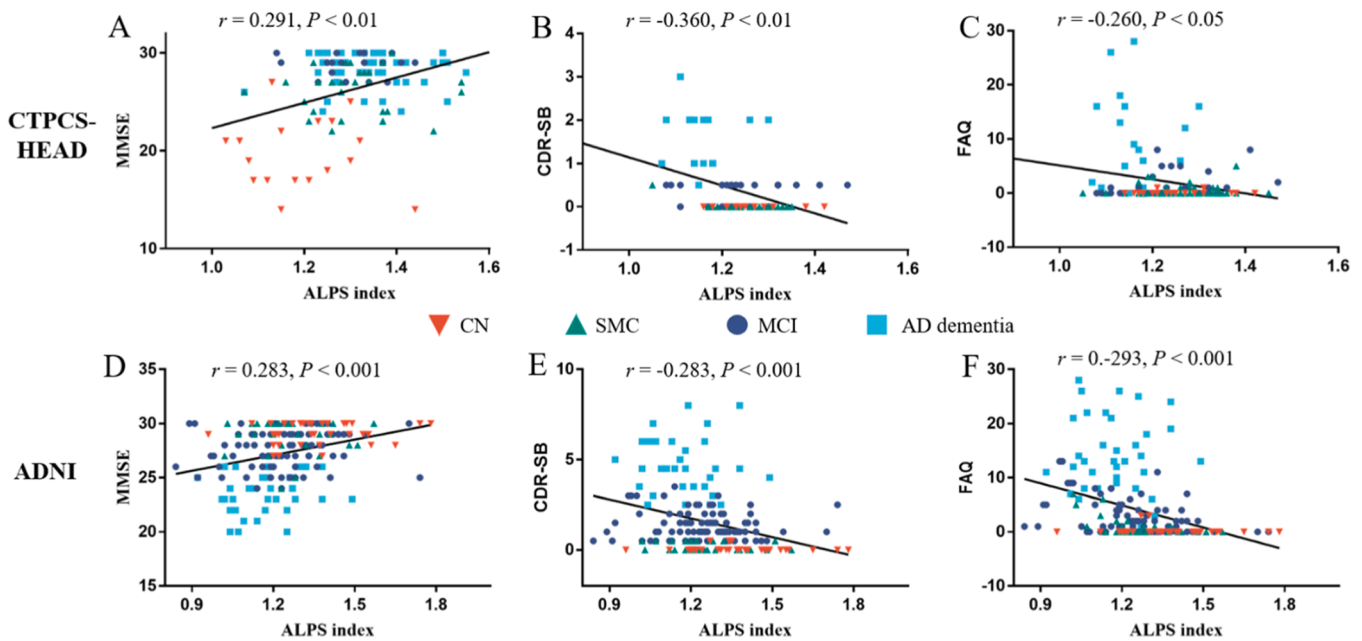


**Table 3**

Comparison of the diffusivities among the study groups for both cohorts.

Cohorts	Parameter	CN	SMC	MCI	AD dementia	$\chi^2$ Value	P Value
ADNI (n = 180)	Dxproj	0.72 (0.59 – 1.04)	0.73 (0.60 – 0.95)	0.63 (0.52 – 0.95)	0.65 (0.52 – 0.94)	<b>44.014</b>	< 0.001
	Dxassoc	0.78 (0.65 – 0.93)	0.78 (0.59 – 0.90)	0.74 (0.59 – 0.96)	0.77 (0.63 – 0.91)	4.664	0.198
	Dyproj	0.66 (0.43 – 0.99)	0.65 (0.51 – 0.90)	0.62 (0.44 – 1.03)	0.69 (0.49 – 0.96)	4.460	0.216
	Dyassoc	1.02 (0.79 – 1.26)	1.01 (0.82 – 1.15)	1.02 (0.69 – 1.27)	1.04 (0.88 – 1.21)	1.958	0.581
	Dzproj	0.96 (0.76 – 1.20)	0.98 (0.85 – 1.23)	0.99 (0.80 – 1.35)	1.01 (0.82 – 1.23)	<b>8.009</b>	<b>0.046</b>
	Dzassoc	0.48 (0.29 – 0.64)	0.55 (0.42 – 0.80)	0.50 (0.35 – 0.73)	0.52 (0.40 – 0.76)	<b>15.979</b>	<b>0.001</b>
CTPCS-HEAD (n = 127)	Dxproj	0.59 (0.53 – 0.65)	0.59 (0.50 – 0.69)	0.58 (0.51 – 0.73)	0.59 (0.49 – 0.77)	2.252	0.522
	Dxassoc	0.64 (0.55 – 0.73)	0.64 (0.54 – 0.77)	0.62 (0.52 – 0.83)	0.63 (0.53 – 0.77)	2.305	0.512
	Dyproj	0.51 (0.41 – 0.61)	0.49 (0.40 – 0.66)	0.51 (0.43 – 0.66)	0.57 (0.49 – 0.69)	<b>28.042</b>	< 0.001
	Dyassoc	0.86 (0.72 – 0.98)	0.82 (0.71 – 1.02)	0.87 (0.72 – 1.07)	0.92 (0.81 – 1.13)	<b>26.877</b>	< 0.001
	Dzproj	0.84 (0.71 – 0.95)	0.85 (0.73 – 1.00)	0.88 (0.76 – 1.08)	0.90 (0.73 – 1.14)	<b>15.140</b>	<b>0.002</b>
	Dzassoc	0.42 (0.38 – 0.47)	0.42 (0.37 – 0.55)	0.42 (0.35 – 0.61)	0.45 (0.36 – 0.59)	5.580	0.134

Note: Unless otherwise specified, data are medians, with ranges in parentheses. Diffusivities are presented as apparent diffusion coefficients ( $\times 10^{-3} \text{ mm}^2/\text{sec}$ ). P values are derived from the comparison between all four groups using the Kruskal-Wallis test.

**Fig. 2.** Correlations between ALPS index and MMSE (A&D), CDR-SB (B&E), and FAQ (C&F) across diagnostic groups for CTPCS-HEAD and ADNI cohorts.**Table 4**

Univariate analysis of the associations between diffusivity, ALPS index, and AD biomarkers (CSF biomarkers for the ADNI cohort and plasma biomarkers for the CTPCS-HEAD cohort).

Parameters	ADNI			CTPCS-HEAD		
	CSF A $\beta$ 42	CSF A $\beta$ 40	CSF pTau	Plasma A $\beta$ 42	Plasma A $\beta$ 40	Plasma pTau
Dxproj	0.122	0.066	-0.114	-0.028	-0.033	-0.292
Dxassoc	0.150	0.128	0.037	0.158	-0.155	0.023
Dyproj	-0.094	-0.064	0.015	-0.200	-0.072	0.442
Dyassoc	-0.218	-0.134	0.006	-0.299	0.039	0.369
Dzproj	-0.316	-0.334	-0.096	-0.207	0.079	0.251**
Dzassoc	-0.076	-0.096	-0.020	-0.064	-0.150	0.215*
ALPS index	0.239*	0.178	-0.059	0.249*	0.038	-0.266

\*  $P < 0.05$ ,\*\*  $P < 0.01$ ,\*\*\*  $P < 0.001$  with FDR correction.

### 3.5. Diagnosis of AD dementia based on ALPS index

The ROC curve was used to evaluate the developed model for differentiating AD dementia from MCI, SMC, and CN (Fig. 3). The areas under the curves (AUC) were 0.802 in the ADNI cohort (Fig. 3A), and 0.783 in the external validation cohort (Fig. 3B), demonstrating that diffusivities and ALPS index diagnosed AD dementia acceptably.

### 3.6. Association between the ALPS index and longitudinal decline of cognition in ADNI cohort

Higher ALPS index levels adjusted for age, sex, education, and APOE4 were associated with less decline in the MMSE score over time ( $\beta = 0.211$ ,  $P < 0.001$ ) for the whole cohort. Specifically, higher ALPS index levels were associated with less decline in the MMSE score over time in A-T + ( $\beta = 0.231$ ,  $P = 0.003$ ), A+T- ( $\beta = 0.350$ ,  $P = 0.001$ ), and A+T+ ( $\beta = 0.623$ ,  $P < 0.001$ ) groups. There was no association between ALPS and cognition decline over time in the A-T- group ( $\beta = 0.028$ ,  $P = 0.451$ ). These results are displayed graphically in Fig. 4A. We further controlled for the GMV ratio in addition to the original confounding variables to study the association between the ALPS index and longitudinal change in the MMSE score, and the result is shown in

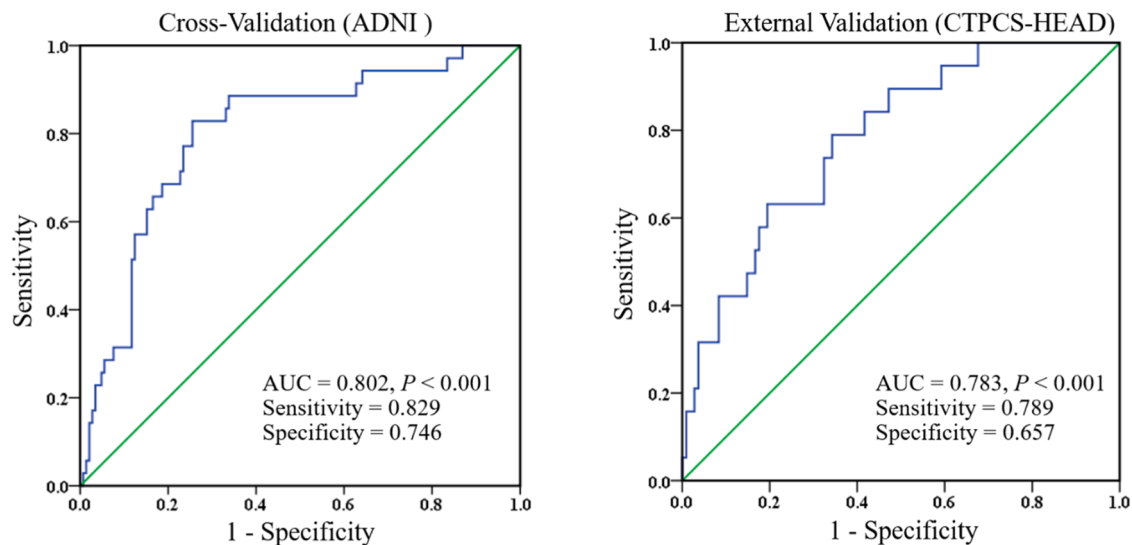


**Fig. 3.** Receiver operation characteristic curve of SVM models based on diffusivities and ALPS index for diagnosis of AD dementia in (A) cross-validation and (B) external validation. Note that the area under the curve (AUC) was 0.802 in the ADNI cohort and 0.783 in the CTPCS-HEAD cohort.

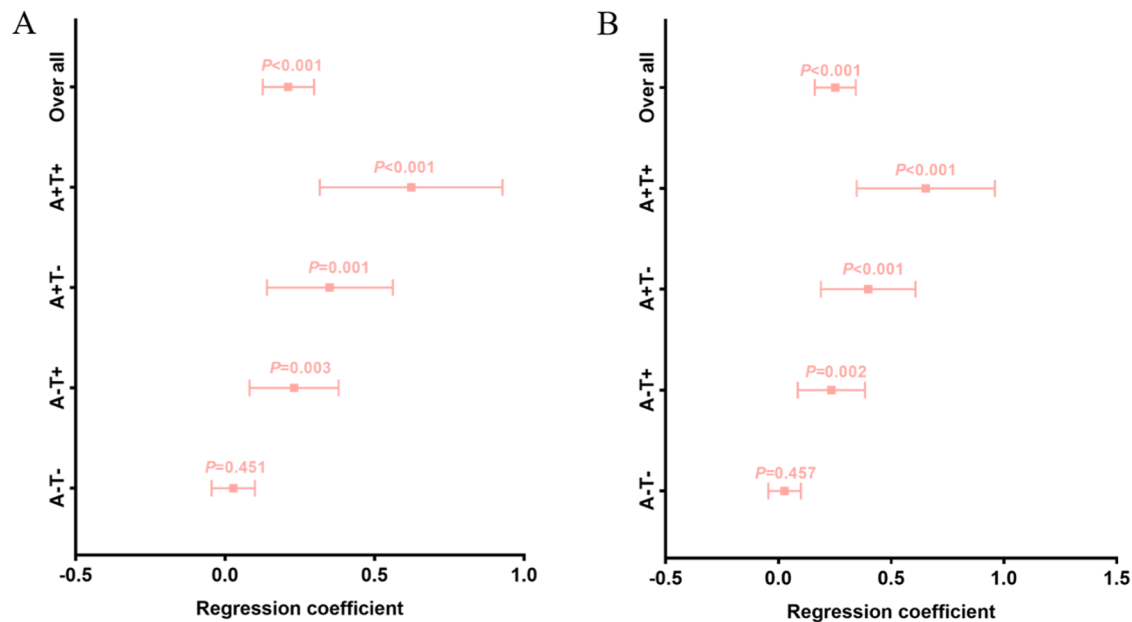


**Fig. 4.** Linear mixed-effects (LME) model to investigate the association between ALPS index and longitudinal MMSE score in various A $\beta$  and tau profiles. (A) All models were adjusted for age, sex, education, and APOE4. (B) All models were additionally adjusted for GMV ratio.

**Fig. 4B.** Higher ALPS index levels were associated with less decline in the MMSE score over time in A-T+ ( $\beta = 0.235$ ,  $P = 0.002$ ), A+T- ( $\beta = 0.398$ ,  $P < 0.001$ ), and A+T+ ( $\beta = 0.653$ ,  $P < 0.001$ ) groups. There was no association between ALPS and cognition decline over time in the A-T- group ( $\beta = 0.027$ ,  $P = 0.457$ ).

3.7. Association between the ALPS index and risk of AD dementia in ADNI cohort

Table 5 provides diffusivities and ALPS index according to conversion status. Conversion group had a lower Dxassoc value, compared to that of nonconversion group ( $P = 0.005$ ). There was a difference between the ALPS index at the time of imaging in the group with MCI who exhibited conversion and that is those who did not (1.19 vs 1.26;  $P = 0.013$ ), and a difference between the CN and the participants with MCI who did not show conversion (1.34 vs. 1.26;  $P = 0.022$ ). There was

**Table 5**  
Comparison of the diffusivities and ALPS index in the group with MCI according to conversion.

Parameter	Conversion Group (n = 27)	Nonconversion Group (n = 50)	Z Value	P Value
Dxproj	0.61 (0.51 – 0.84)	0.64 (0.54 – 0.95)	1.591	0.112
Dxassoc	0.71 (0.60 – 0.86)	0.76 (0.58 – 0.95)	2.808	<b>0.005*</b>
Dyproj	0.62 (0.54 – 1.03)	0.63 (0.44 – 0.87)	0.619	0.536
Dyassoc	1.05 (0.83 – 1.20)	1.01 (0.69 – 1.27)	1.505	0.132
Dzproj	0.97 (0.84 – 1.35)	0.99 (0.80 – 1.29)	1.078	0.281
Dzassoc	0.49 (0.35 – 0.73)	0.50 (0.38 – 0.66)	0.171	0.864
ALPS index	1.19 (0.91 – 1.44)	1.26 (0.84 – 1.74)	2.477	<b>0.013*</b>

Note: Unless otherwise specified, data are medians, with ranges in parentheses. Diffusivities are presented as apparent diffusion coefficients ( $\times 10^{-3}$  mm<sup>2</sup>/sec). P values were derived with the use of the Mann-Whitney U test.

no evidence of a difference in the ALPS index between the participants with MCI who developed conversion and the group with AD dementia (1.19 vs. 1.18,  $P = 0.870$ ). The estimated conversion-free probability in participants with MCI is shown in Fig. 5. The risk of AD dementia conversion in participants with MCI decreased with increasing ALPS index (hazard ratio, 0.76 per 0.1 increase in ALPS index [95 % CI: 0.61, 0.94];  $P = 0.014$ ).

#### 4. Discussion

In this study, we found that the ALPS index reflecting ISF dynamics was decreased in the group with AD dementia compared with CN, SMC, and MCI groups in both cohorts. Higher ALPS index levels were associated with less decline in MMSE score and a lower risk of MCI to AD dementia conversion. These findings demonstrated that glymphatic dysfunction may contribute to the conversion from MCI to AD dementia. Preserved ISF dynamics with a higher ALPS index may act as a neuroprotective mechanism against the progression of AD.

The DTI-ALPS method noninvasively quantifies ISF dynamics linked to glymphatic function (Taoka et al., 2017; Hsu et al., 2023; Steward et al., 2021). A prior human study validated DTI-ALPS by correlating the ALPS index with delayed glymphatic clearance observed through intrathecal contrast agent injections (Zhang et al., 2021). Our findings further verify the method by showing an age-dependent trend in the ALPS index consistent with earlier preclinical and human studies. The ALPS index has also been shown to have high reproducibility and strong intra- and interobserver agreement. Given that DTI can be completed in minutes, the ALPS index was used in this study to predict the development of AD. For DTI data, there was geometric distortion along the phase-encoding direction and motion across different diffusion directions. Due to the lack of reverse phase-encoding data for correction of geometric distortion, we excluded the participants with severe distortion by visual evaluation. We performed head motion-corrected and participants with head motion > 2 mm translation and/or > 2 rotation in any direction were excluded.

Glymphatic dysfunction contributes to the development of AD dementia by impairing the clearance of A $\beta$  and tau proteins from the brain. Recent studies have reported a lower ALPS index in patients with AD dementia compared to cognitively normal individuals (Kamagata et al., 2022; Ota et al., 2022). Hus et al. also found that glymphatic activity significantly mediates the relationship between A $\beta$  and tau protein burden and cognitive dysfunction in AD (Hsu et al., 2023). However, the

connection between the ALPS index, cognition, and the risk of AD dementia conversion has not been thoroughly investigated. Here we observed a lower ALPS index in the AD dementia group compared to the other three groups across both cohorts, indicating reduced ISF dynamics in the later stages of AD. In contrast, diffusivities along the y-axis and z-axis in association and projection neural fibers were higher in the AD dementia group, suggesting white matter degeneration or variations in white matter integrity (Taoka et al., 2017; Bae et al., 2021). The degeneration of white matter will affect the accuracy of ALPS calculation. According to a previous study (Benitez et al., 2018), the FA threshold of 0.3 was applied in this work to eliminate the impact of white matter microstructure impairment. A lower FA value could not effectively eliminate white matter microstructure impairment, while a higher FA value will result in limited voxels for ALPS calculation. Diffusivities along the x-axis, which align with perivascular water flow, were influenced by both ISF dynamic changes and white matter microstructure impairment. Since these factors have opposing effects on x-axis diffusivities, Dxproj and Dxassoc do not directly reflect ISF dynamics. The ALPS index, as defined in Eq. (1), partially mitigates the impact of white matter microstructure impairment and more accurately reflects ISF dynamics. Therefore, we investigated the association between the ALPS index, cognition, and the risk of AD dementia conversion in this study.

Previous studies have shown that the ALPS index had significant positive correlations with cognitive scores in patients with AD dementia, MCI individuals, and elderly CN individuals (Taoka et al., 2017; Steward et al., 2021; Siow et al., 2022). Our findings align with these results, demonstrating significant positive correlations between the ALPS index and MMSE scores in both cohorts. Additionally, we observed significant negative correlations between the ALPS index and both CDR-SB and FAQ scores. The CDR-SB score assesses six key domains (memory, orientation, judgment, problem-solving, community affairs, home and hobbies, and personal care), with higher scores indicating greater impairment (van Dyck et al., 2023). The FAQ score evaluates participants' abilities in instrumental activities of daily living, where higher scores indicate greater dependence (González et al., 2022). The association between the ALPS index and these cognitive measures, along with a higher AUC for AD diagnosis in cross-cohort validation using SVM, suggests that the ALPS index has strong potential as a biomarker for AD diagnosis and cognitive prediction.

We further explored the relationship between the ALPS index and cognitive decline, particularly the decline in MMSE scores, and its

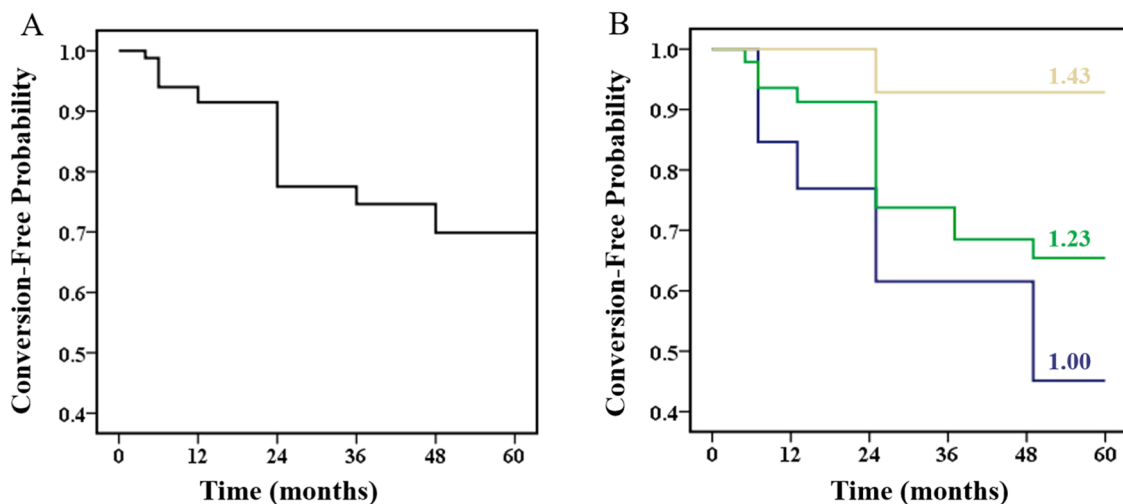


**Fig. 5.** Cox regression analysis of the risk of AD dementia conversion in participants with MCI. (A) The survival probability graph from Cox regression analysis of a total of 77 participants in the group with MCI shows the conversion-free probability with the median analysis along the perivascular space (ALPS) index. (B) The survival graph shows the conversion-free probability according to the specific ALPS index. The conversion-free probability is higher with higher ALPS index (values shown on the graph).

association with conversion to AD dementia. Our results indicate that higher ALPS index levels are associated with less cognitive decline and a lower risk of conversion from MCI to AD dementia. These findings support the hypothesis that the ALPS index could serve as a biomarker for AD progression. Specifically, ALPS index levels were significantly associated with cognitive decline in the A-T+, A+T-, and A+T+ groups, but not in the A-T- group, indicating the index's sensitivity to predicting cognitive decline in A+ or T+ stages. Given that GM atrophy is an independent predictor of cognitive decline (Malpetti et al., 2020) and is significantly correlated with the ALPS index (Hsu et al., 2023), our findings persisted even after adjusting for GMV ratio, further verifying the ALPS index's value in predicting AD development.

Sleep quality decreases as a function of normal aging and insomnia is more frequent for patients with AD (Nedergaard and Goldman, 2020). The impairment in sleep quality for patients with AD may be involved in the accelerated course of neurodegenerative disease and sharply diminished brain ISF dynamics and its export of protein waste, resulting in reduced ALPS index (Nedergaard and Goldman, 2020). On the other hand, vascular risk directly results in the accumulation of aberrant proteins and subsequently reduces ISF dynamic in the brain (Romay et al., 2024). These may explain our finding that the ALPS index is positively correlated with CSF A $\beta$ 42 levels and aligns with previous research showing a negative relationship between the ALPS index and regional standardized uptake value ratios in A $\beta$ -PET images (Hsu et al., 2023). After the CSF-ISF exchange, the resulting mixture flows along perivascular or perineural tracts to downstream lymphatic vessels or draining veins (Reeves et al., 2020; Benveniste et al., 2019), reducing the amount of A $\beta$  entering the bloodstream. This could account for the observed decrease in plasma A $\beta$ 42 levels in the AD dementia group and the positive correlation between the ALPS index and plasma A $\beta$ 42 levels. There was no significant difference in plasma A $\beta$ 40 levels across diagnostic groups, and thus no association with the ALPS index. These findings further support the potential of plasma A $\beta$ 42 levels as a biomarker for AD diagnosis and glymphatic impairment.

This study had several limitations. First, the lack of follow-up data in the CTPCS-HEAD cohort prevented further validation of the ALPS index as a predictor of cognitive decline and AD dementia conversion within this group. Second, we did not account for the influence of sleep parameters, cardiovascular factors, or medications on the glymphatic system, all of which could affect perivascular glymphatic flow in patients. Lastly, the ALPS index serves as a global biomarker for the entire brain, rather than as a regional functional measure. Given that early-stage AD is characterized by focal rather than widespread brain changes, the ALPS index reflecting whole brain ISF dynamic may have limited sensitivity in detecting these early alterations.

## 5. Conclusion

The ALPS index reflecting ISF dynamics associated with glymphatic activity has great potential in AD dementia diagnosis. Higher ALPS index levels are associated with less decline in MMSE score and a lower risk of AD dementia conversion. These findings suggest that the ALPS index may provide a useful AD progression or treatment biomarker.

## Ethical approval

This study was approved by the Ethics Committee of Hainan General Hospital of Hainan Medical University.

## CRediT authorship contribution statement

**Zhou Juan Helen:** Writing – review & editing. **Wang Yi:** Writing – review & editing, Methodology. **Wang Xiaoyi:** Writing – review & editing, Data curation. **Zhang Kun:** Data curation. **Huang Weiyuan:** Writing – review & editing. **Zhou Liangdong:** Writing – review & editing, Methodology. **Chen Huijuan:** Methodology, Data curation. **Liu**

**Tao:** Writing – review & editing, Project administration, Methodology, Investigation. **Guo Yihao:** Writing – review & editing, Writing – original draft, Methodology, Investigation, Formal analysis, Conceptualization. **Chen Feng:** Writing – review & editing, Project administration, Methodology, Funding acquisition.

## Declaration of Competing Interest

The authors declare that they have no conflict of interest.

## Acknowledgments

This project was supported by the Key Science and Technology Project of Hainan Province (ZDYF2024SHFZ058), the National Natural Science Foundation of China (82271977), the Hainan Province 'Nanhai Rising Star' Healthcare Talent Platform Project (NHXX-WJW-2023009), the Hainan Academician Innovation Platform Fund, and the Hainan Province Clinical Medical Center.

The authors want to acknowledge the study participants and all the investigators involved in the Alzheimer's Disease Neuroimaging Initiative (ADNI). Parts of the data used in preparation of this manuscript were obtained from the ADNI database (adni.loni.usc.edu). As such, the investigators within the ADNI study contributed to the design and implementation of ADNI and/or provided data but did not participate in analysis or writing of this article. Data collection and sharing for this project was funded by the ADNI (National Institutes of Health Grant U01 AG024904) and DOD ADNI (Department of Defense award number W81XWH-12-2-0012). ADNI is funded by the National Institute on Aging, the National Institute of Biomedical Imaging and Bioengineering, and through generous contributions from the following: AbbVie, Alzheimer's Association; Alzheimer's Drug Discovery Foundation; Araclon Biotech; BioClinica, Inc.; Biogen; Bristol-Myers Squibb Company; CereSpir, Inc.; Cogstate; Eisai Inc.; Elan Pharmaceuticals, Inc.; Eli Lilly and Company; EuroImmun; F. Hoffmann-La Roche Ltd and its affiliated company Genentech, Inc.; Fujirebio; GE Healthcare; IXICO Ltd.; Janssen Alzheimer Immunotherapy Research & Development, LLC.; Johnson & Johnson Pharmaceutical Research & Development LLC.; Lumosity; Lundbeck; Merck & Co., Inc.; Meso Scale Diagnostics, LLC.; NeuroRx Research; Neurotrack Technologies; Novartis Pharmaceuticals Corporation; Pfizer Inc.; Piramal Imaging; Servier; Takeda Pharmaceutical Company; and Transition Therapeutics. The Canadian Institutes of Health Research is providing funds to support ADNI clinical sites in Canada. Private sector contributions are facilitated by the Foundation for the National Institutes of Health ([www.fnih.org](http://www.fnih.org)). The grantee organization is the Northern California Institute for Research and Education, and the study is coordinated by the Alzheimer's Therapeutic Research Institute at the University of Southern California. ADNI data are disseminated by the Laboratory for Neuro Imaging at the University of Southern California.

## Consent to participate

Informed consent was obtained from all individual participants included in the study.

## Consent for publication

All of the authors agreed to submit the paper for publication.

## Data availability

Data will be made available on request.



## References

- Aisen, P.S., Petersen, R.C., Donohue, M., Weiner, M.W., 2015. Alzheimer's disease neuroimaging initiative 2 clinical core: progress and plans. *Alzheimer's Dement.: J. Alzheimer's S. Assoc.* 11 (7), 734–739. <https://doi.org/10.1016/j.jalz.2015.05.005>.
- Albert, M.S., DeKosky, S.T., Dickson, D., Dubois, B., Feldman, H.H., Fox, N.C., Gamst, A., Holtzman, D.M., Jagust, W.J., Petersen, R.C., et al., 2011. The diagnosis of mild cognitive impairment due to Alzheimer's disease: recommendations from the National Institute on Aging-Alzheimer's Association workgroups on diagnostic guidelines for Alzheimer's disease. *Alzheimer's Dement.: J. Alzheimer's S. Assoc.* 7 (3), 270–279. <https://doi.org/10.1016/j.jalz.2011.03.008>.
- Bae, Y.J., Choi, B.S., Kim, J.M., Choi, J.H., Cho, S.J., Kim, J.H., 2021. Altered glymphatic system in idiopathic normal pressure hydrocephalus. *Park. Relat. Disord.* 82, 56–60. <https://doi.org/10.1016/j.parkrel.2020.11.009>.
- Basaia, S., Agosta, F., Wagner, L., Canu, E., Magnani, G., Santangelo, R., Filippi, M., 2019. Automated classification of Alzheimer's disease and mild cognitive impairment using a single MRI and deep neural networks. *Neuroimage Clin.* 21, 101645. <https://doi.org/10.1016/j.nicl.2018.101645>.
- Benitez, A., Jensen, J.H., Falangola, M.F., Nietert, P.J., Helpert, J.A., 2018. Modeling white matter tract integrity in aging with diffusional kurtosis imaging. *Neurobiol. Aging* 70, 265–275. <https://doi.org/10.1016/j.neurobiolaging.2018.07.006>.
- Benveniste, H., Liu, X., Koundal, S., Sanggaard, S., Lee, H., Wardlaw, J., 2019. The glymphatic system and waste clearance with brain aging: a review. *Gerontology* 65 (2), 106–119. <https://doi.org/10.1159/000490349>.
- Bittner, T., Zetterberg, H., Teunissen, C.E., Ostlund Jr., R.E., Militello, M., Andreasson, U., Hübner, I., Gibson, D., Chu, D.C., Eichenlaub, U., et al., 2016. Technical performance of a novel, fully automated electrochemoluminescence immunoassay for the quantitation of  $\beta$ -amyloid (1–42) in human cerebrospinal fluid. *Alzheimer's Dement.: J. Alzheimer's S. Assoc.* 12 (5), 517–526. <https://doi.org/10.1016/j.jalz.2015.09.009>.
- Bondi, M.W., Edmonds, E.C., Jak, A.J., Clark, L.R., Delano-Wood, L., McDonald, C.R., Nation, D.A., Libon, D.J., Au, R., Galasko, D., et al., 2014. Neuropsychological criteria for mild cognitive impairment improves diagnostic precision, biomarker associations, and progression rates. *J. Alzheimer's Dis.* 42 (1), 275–289. <https://doi.org/10.3233/jad-140276>.
- Bucci, M., Chiotis, K., Nordberg, A., Alzheimer's Disease Neuroimaging I., 2021. Alzheimer's disease profiled by fluid and imaging markers: tau PET best predicts cognitive decline. *Mol. Psychiatry* 26 (10), 5888–5898. <https://doi.org/10.1038/s41302-021-01263-2>.
- Cao, X., Xu, H., Feng, W., Su, D., Xiao, M., 2018. Deletion of aquaporin-4 aggravates brain pathology after blocking of the meningeal lymphatic drainage. *Brain Res. Bull.* 143, 83–96. <https://doi.org/10.1016/j.brainresbull.2018.10.007>.
- van Dyck, C.H., Swanson, C.J., Aisen, P., Bateman, R.J., Chen, C., Gee, M., Kanekiyo, M., Li, D., Rhyderman, L., Cohen, S., et al., 2023. Lecanemab in Early Alzheimer's Disease. *N. Engl. J. Med.* 388 (1), 9–21. <https://doi.org/10.1056/NEJMoa2212948>.
- Eide, P.K., Ringstad, G., 2015. MRI with intrathecal MRI gadolinium contrast medium administration: a possible method to assess glymphatic function in human brain. *Acta Radiol. Open* 4 (11), 2058460115609635. <https://doi.org/10.1177/2058460115609635>.
- González, D.A., Gonzales, M.M., Resch, Z.J., Sullivan, A.C., Soble, J.R., 2022. Comprehensive Evaluation of the Functional Activities Questionnaire (FAQ) and Its Reliability and Validity. *Assessment* 29 (4), 748–763. <https://doi.org/10.1177/1073191121991215>.
- Haller, S., Moy, L., Anzai, Y., 2024. Evaluation of diffusion tensor imaging analysis along the perivascular space as a marker of the glymphatic system. *Radiology* 310 (1), e232899. <https://doi.org/10.1148/radiol.232899>.
- Hsu, J.L., Wei, Y.C., Toh, C.H., Hsiao, I.T., Lin, K.J., Yen, T.C., Liao, M.F., Ro, L.S., 2023. Magnetic resonance images indicate that glymphatic alterations mediate cognitive dysfunction in Alzheimer disease. *Ann. Neurol.* 93 (1), 164–174. <https://doi.org/10.1002/ana.26516>.
- Iliff, J.J., Wang, M., Liao, Y., Plogg, B.A., Peng, W., Gundersen, G.A., Benveniste, H., Vates, G.E., Deane, R., Goldman, S.A., et al., 2012. A paravascular pathway facilitates CSF flow through the brain parenchyma and the clearance of interstitial solutes, including amyloid  $\beta$ . *Sci. Transl. Med.* 4 (147), 147ra111. <https://doi.org/10.1126/scitranslmed.3003748>.
- Iliff, J.J., Lee, H., Yu, M., Feng, T., Logan, J., Nedergaard, M., Benveniste, H., 2013. Brain-wide pathway for waste clearance captured by contrast-enhanced MRI. *J. Clin. Invest.* 123 (3), 1299–1309. <https://doi.org/10.1172/jci67677>.
- Jack Jr., C.R., Knopman, D.S., Jagust, W.J., Petersen, R.C., Weiner, M.W., Aisen, P.S., Shaw, L.M., Vemuri, P., Wiste, H.J., Weigand, S.D., et al., 2013. Tracking pathophysiological processes in Alzheimer's disease: an updated hypothetical model of dynamic biomarkers. *Lancet Neurol.* 12 (2), 207–216. [https://doi.org/10.1016/s1474-4422\(12\)70291-0](https://doi.org/10.1016/s1474-4422(12)70291-0).
- Jack Jr., C.R., Bennett, D.A., Blennow, K., Carrillo, M.C., Dunn, B., Haeberlein, S.B., Holtzman, D.M., Jagust, W., Jessen, F., Karlawish, J., et al., 2018. NIA-AA Research Framework: Toward a biological definition of Alzheimer's disease. *Alzheimer's Dement.: J. Alzheimer's S. Assoc.* 14 (4), 535–562. <https://doi.org/10.1016/j.jalz.2018.02.018>.
- Kamagata, K., Andica, C., Takabayashi, K., Saito, Y., Taoka, T., Nozaki, H., Kikuta, J., Fujita, S., Hagiwara, A., Kamiya, K., et al., 2022. Association of MRI indices of glymphatic system with amyloid deposition and cognition in mild cognitive impairment and Alzheimer disease. *Neurology* 99 (24), e2648–e2660. <https://doi.org/10.1212/wnl.00000000000201300>.
- Karran, E., Mercken, M., De Strooper, B., 2011. The amyloid cascade hypothesis for Alzheimer's disease: an appraisal for the development of therapeutics. *Nat. Rev. Drug Discov.* 10 (9), 698–712. <https://doi.org/10.1038/nrd3505>.
- Li, T.R., Yao, Y.X., Jiang, X.Y., Dong, Q.Y., Yu, X.F., Wang, T., Cai, Y.N., Han, Y., 2022.  $\beta$ -Amyloid in blood neuronal-derived extracellular vesicles is elevated in cognitively normal adults at risk of Alzheimer's disease and predicts cerebral amyloidosis. *Alzheimer's Res. Ther.* 14 (1), 66. <https://doi.org/10.1186/s13195-022-01010-x>.
- Malpetti, M., Kievit, R.A., Passamonti, L., Jones, P.S., Tsvetanov, K.A., Rittman, T., Mak, E., Nicastro, N., Bevan-Jones, W.R., Su, L., et al., 2020. Microglial activation and tau burden predict cognitive decline in Alzheimer's disease. *Brain* 143 (5), 1588–1602. <https://doi.org/10.1093/brain/awaa088>.
- Mayo, C.D., Mazerolle, E.L., Ritchie, L., Fisk, J.D., Gawryluk, J.R., 2017. Longitudinal changes in microstructural white matter metrics in Alzheimer's disease. *Neuroimage Clin.* 13, 330–338. <https://doi.org/10.1016/j.nicl.2016.12.012>.
- McKhann, G.M., Knopman, D.S., Chertkow, H., Hyman, B.T., Jack Jr., C.R., Kawas, C.H., Klunk, W.E., Koroshetz, W.J., Manly, J.J., Mayeux, R., et al., 2011. The diagnosis of dementia due to Alzheimer's disease: recommendations from the National Institute on Aging-Alzheimer's Association workgroups on diagnostic guidelines for Alzheimer's disease. *Alzheimer's Dement.: J. Alzheimer's S. Assoc.* 7 (3), 263–269. <https://doi.org/10.1016/j.jalz.2011.03.005>.
- Nedergaard, M., Goldman, S.A., 2020. Glymphatic failure as a final common pathway to dementia. *Sci. (N. Y., NY)* 370 (6512), 50–56. <https://doi.org/10.1126/science.abb8739>.
- Oshio, K., 2023. What Is the "Glymphatic System"? *Magn. Reson. Med. Sci.* 22 (1), 137–141. <https://doi.org/10.2463/mrms.bc.2021-0059>.
- Ota, M., Sato, N., Nakaya, M., Shigemoto, Y., Kimura, Y., Chiba, E., Yokoi, Y., Tsukamoto, T., Matsuda, H., 2022. Relationships between the deposition of amyloid-beta and tau protein and glymphatic system activity in Alzheimer's disease: diffusion tensor image study. *J. Alzheimers Dis.* 90 (1), 295–303. <https://doi.org/10.3233/JAD-220534>.
- Patel, T.K., Habimana-Griffin, L., Gao, X., Xu, B., Achilefu, S., Alitalo, K., McKee, C.A., Sheehan, P.W., Musiek, E.S., Xiong, C., et al., 2019. Dural lymphatics regulate clearance of extracellular tau from the CNS. *Mol. Neurodegener.* 14 (1), 11. <https://doi.org/10.1186/s13024-019-0312-x>.
- Petersen, R.C., Aisen, P.S., Beckett, L.A., Donohue, M.C., Gamst, A.C., Harvey, D.J., Jack Jr., C.R., Jagust, W.J., Shaw, L.M., Toga, A.W., et al., 2010. Alzheimer's Disease Neuroimaging Initiative (ADNI): clinical characterization. *Neurology* 74 (3), 201–209. <https://doi.org/10.1212/WNL.0b013e3181cb3e25>.
- Reeves, B.C., Karimy, J.K., Kundishora, A.J., Mestre, H., Cerri, H.M., Matouk, C., Alper, S.L., Lundgaard, L., Nedergaard, M., Kahle, K.T., 2020. Glymphatic system impairment in Alzheimer's disease and idiopathic normal pressure hydrocephalus. *Trends Mol. Med.* 26 (3), 285–295. <https://doi.org/10.1016/j.molmed.2019.11.008>.
- Romay, M.C., Knutsen, R.H., Ma, F., Mompeón, A., Hernandez, G.E., Salvador, J., Mirkov, S., Batra, A., Sullivan, D.P., Procissi, D., et al., 2024. Age-related loss of Notch3 underlies brain vascular contractility deficiencies, glymphatic dysfunction, and neurodegeneration in mice. *J. Clin. Invest.* 134 (2). <https://doi.org/10.1172/jci66134>.
- Scheltens, P., De Strooper, B., Kivipelto, M., Holstege, H., Chételat, G., Teunissen, C.E., Cummings, J., van der Flier, W.M., 2021. Alzheimer's disease. *Lancet (Lond., Engl.)* 397 (10284), 1577–1590. [https://doi.org/10.1016/s0140-6736\(20\)32205-4](https://doi.org/10.1016/s0140-6736(20)32205-4).
- Siow, T.Y., Toh, C.H., Hsu, J.L., Liu, G.H., Lee, S.H., Chen, N.H., Fu, C.J., Castillo, M., Fang, J.T., 2022. Association of sleep, neuropsychological performance, and gray matter volume with glymphatic function in community-dwelling older adults. *Neurology* 98 (8), e829–e838. <https://doi.org/10.1212/WNL.0000000000003215>.
- Steward, C.E., Venkatraman, V.K., Lui, E., Malpas, C.B., Ellis, K.A., Cyarto, E.V., Vivash, L., O'Brien, T.J., Velakoulis, D., Ames, D., et al., 2021. Assessment of the DTI-ALPS Parameter Along the Perivascular Space in Older Adults at Risk of Dementia. *J. Neuroimaging: Off. J. Am. Soc. Neuroimaging* 31 (3), 569–578. <https://doi.org/10.1111/jon.12837>.
- Taoka, T., Naganawa, S., 2020b. Glymphatic imaging using MRI. *J. Magn. Reson. Imaging* 51 (1), 11–24. <https://doi.org/10.1002/jmri.26892>.
- Taoka, T., Naganawa, S., 2020a. Neurofluid dynamics and the glymphatic system: a neuroimaging perspective. *Korean J. Radiol.* 21 (11), 1199–1209. <https://doi.org/10.3348/kjr.2020.0042>.
- Taoka, T., Masutani, Y., Kawai, H., Nakane, T., Matsuoka, K., Yasuno, F., Kishimoto, T., Naganawa, S., 2017. Evaluation of glymphatic system activity with the diffusion MR technique: diffusion tensor image analysis along the perivascular space (DTI-ALPS) in Alzheimer's disease cases. *Jpn J. Radio.* 35 (4), 172–178. <https://doi.org/10.1007/s11604-017-0617-z>.
- Yokota, H., Vijayasarathi, A., Cecik, M., Hirata, Y., Linetsky, M., Ho, M., Kim, W., Salamon, N., 2019. Diagnostic performance of glymphatic system evaluation using diffusion tensor imaging in idiopathic normal pressure hydrocephalus and mimickers. *Curr. Gerontol. Geriatr. Res.* 2019, 5675014. <https://doi.org/10.1155/2019/5675014>.
- Zhang, W., Zhou, Y., Wang, J., Gong, X., Chen, Z., Zhang, X., Cai, J., Chen, S., Fang, L., Sun, J., et al., 2021. Glymphatic clearance function in patients with cerebral small vessel disease. *Neuroimage* 238, 118257. <https://doi.org/10.1016/j.neuroimage.2021.118257>.
- Zhou, L., Nguyen, T.D., Chiang, G.C., Wang, X.H., Xi, K., Hu, T.W., Tanzi, E.B., Butler, T. A., de Leon, M.J., Li, Y., 2024. Parenchymal CSF fraction is a measure of brain glymphatic clearance and positively associated with amyloid beta deposition on PET. *Alzheimer's Dement.: J. Alzheimer's S. Assoc.* 20 (3), 2047–2057. <https://doi.org/10.1002/alz.13659>.